

Some comments on the mechanics of thermal buckling

Synopsis

Last year's hot summer saw an increased number of reported buckling failures of rail track. Similar restrained thermal buckling problems are experienced in concrete road pavements, buried land-based and subsea pipelines, bituminous pavements, parquet and laminate floors, the earth's crust and even ice sheets. For all of these phenomena the underlying mechanics is very closely related, of considerable analytical challenge in its complexity and yet capable of a fairly simple interpretation. The following short note outlines an alternative way of representing the non-linear buckling behaviour that has the merit of being both simple and yet capable of producing explicit analytical representations of the imperfection sensitive buckling loads. Since a similar form of buckling can be exhibited in many commonly employed structural components, for example in sandwich composite panels, this approach may be of interest.

Introduction

The hot summer weather of 2003 brought with it an increased frequency of railway line buckles with the consequent inconvenience to passengers of either cancelled or restricted speed services. If it was simply a question of the 'wrong sort of heat', as the tabloids are so keen to put it, then the patient public would be quite justified in being pretty aggrieved. In fact the phenomenon of thermal buckling of systems like rail tracks is a problem of considerable mechanical complexity. Temperatures required to cause buckling are critically dependent upon the levels and shapes of any pre-existing geometric imperfections, with the non-linear snap buckling behaviour being closer to that experienced in thin shells than that normally associated with what are essentially columns. Add to this the importance of the friction between the track and the sub-grade in both the longitudinal and lateral directions and it is understandable why such failures are not uncommon.

The complexity of the behaviour was brought home to the author during his one and only period of sabbatical leave in Princeton in 1979. By chance I was allocated the office of Professor Arnold Kerr who was coincidentally also on a period of leave. At the time Kerr was one of the few people publishing on the phenomena associated with the buckling of rail track and later road pavements, so that I had the benefit of being able to browse through the many reprints on his office shelves. Deterred by the analytical complexity of these articles, and in any case being rather preoccupied with problems associated with the buckling of concrete cooling towers, I gave the problem little more thought for the next 20 years. It was just a few years ago that I was involved with the examination of a thesis concerned with the closely related phenomenon of thermal uplift buckling of subsea pipelines, carrying high temperature oil or gas, when I was forced to reconsider this problem. In the course of examining this work I had occasion to develop what for me seemed a simpler way of thinking about the problem. Since this alternative approach depends upon fairly straightforward mechanics, but produces some simple and elegant closed form solutions, it may be of interest to a wider readership than just railway engineers. For in applications as diverse as concrete road pavements, pipelines, blistering of bituminous pavements surfaces, uplift of wood block floors and especially the thin laminates currently so fashionable in home improvements, blistering of the skins of sandwich composites, ...very similar behaviour is experienced.

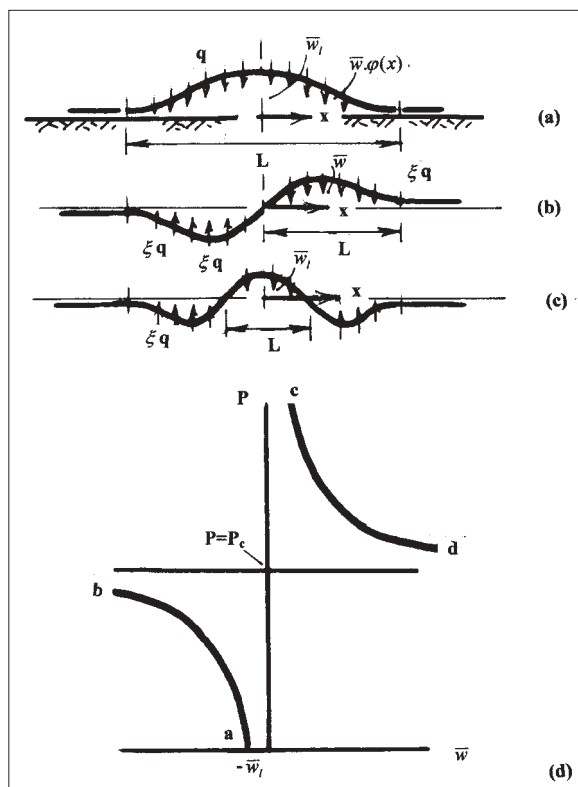
Mechanics of behaviour

If a long continuous railway line, pipeline, concrete pavement, ...is subject to an increase in temperature, but restrained longitudinally from expansion, an axial compression will develop. Under certain conditions these axial compressions may become great enough to cause either an upheaval buckling or a lateral buckling against the restraint provided by the foundation with which it interacts. For generality a railway line, pipeline, pavement, or what ever, will in the following be referred to as a restrained column. The restraint could come from the foundation itself for the case of upheaval buckling, or it could be the friction between the column and the foundation for the case of lateral buckling. Once mobilised the column over the buckled wavelength will be opposed by the weight of the column for upheaval and the dynamic friction for lateral buckling. Although the modes will be affected by whether it is upheaval or lateral buckling the essential mechanics is the same.

Column model of buckling: The classical problem of restrained thermal buckling may be treated on the basis of simple column behaviour. It is well known that a column with an imperfection of magnitude, $-\bar{w}_1$, having the same form as the critical mode will exhibit a non-linear response

$$\bar{w} = \frac{1}{1 - \frac{P}{P_c}} \cdot (-\bar{w}_1) \quad \dots(1)$$

where \bar{w} is the amplitude of deformation at the current level of axial load P and P_c is the critical load in a mode having the form $\varphi(x)$. For upheaval buckling from an essentially rigid foundation, the mode form would be that shown in Fig 1(a); this is the form of buckling exhibited by a clamped column. For lateral buckling the mode form might be one or other of the modes shown in Fig 1(b) and (c). What is different from the equivalent column buckling is that in this case



Prof. James G. A. Croll

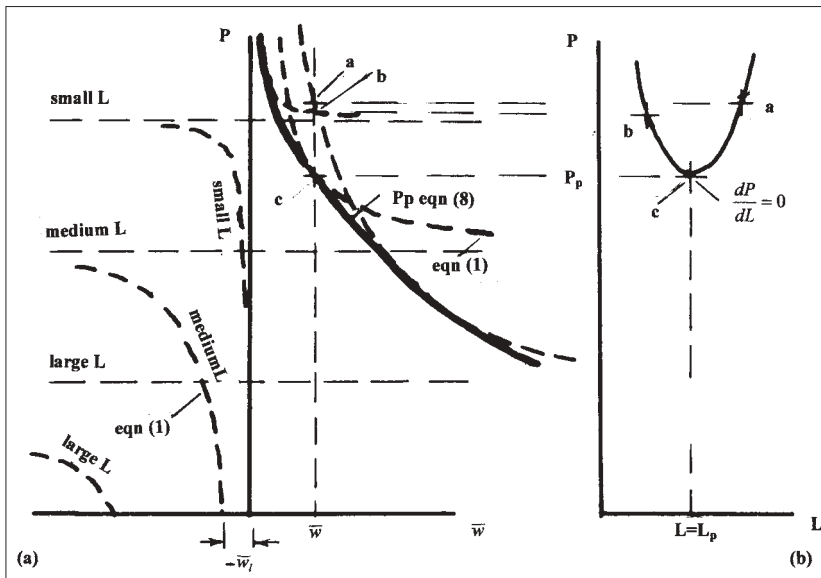
BE, PhD, CEng, FREng, FStructE, FICE

Department of Civil and Environmental Engng, University College London

Received: 01/04
Accepted: 11/04
Keywords: Buckling, Modelling, Columns, Temperatures, Pavements, Railway track

© James G. A. Croll

Fig 1. Mode shapes for (a) upheaval buckling (b) (c) lateral buckling, and (d) the underlying column response



a positive deformation is opposed by a line load equal to the self weight, q , of the column, or in the case of lateral buckling by the kinematic friction line load force, ξq . These opposing forces would in the absence of the restraint produce deformation in the opposite direction to those of the current deformation, which means that they are equivalent to a loading imperfection, $-\bar{w}$, producing the response shown in Fig 1(d). As a result of the restraint a negative deformation associated with path 'a-b' is not possible, so that the only relevant displacement is that of the path 'c-d'. These so-called complementary equilibrium paths associated with eqn (1) when $P > P_c$ are usually of little relevance for column buckling. The equilibrium states on the path 'c-d' are unstable and consequently not able to be observed in any realistic experiment. For thermal buckling however, they are of crucial importance.

Propagation of prestrained buckling: The classic problem of how the buckle of a thermally restrained column propagates may be modelled on the basis of eqn (1) in the following way. Imagine that at a certain stage of the uplift buckling of Fig 1(a) the deformation has reached the level, \bar{w} . As suggested in Fig 2(a) there will be an infinite number of wavelengths for which this level of deformation is possible. Each will correspond with different imperfection amplitudes proportional to the 4th power of the current wavelength L and each wavelength will have a critical load inversely proportional to the 2nd power of L . The loading imperfection can be thought of as the downward deformation that the column would experience if it were not prevented from doing so by the assumed rigid foundation. A small L will have a small loading imperfection, $-\bar{w}_1$, but a large critical load, P_c ;

Fig 2. Equivalent loading imperfections showing (a) the behaviour with various uplift wavelengths, and (b) the minimising or propagation condition

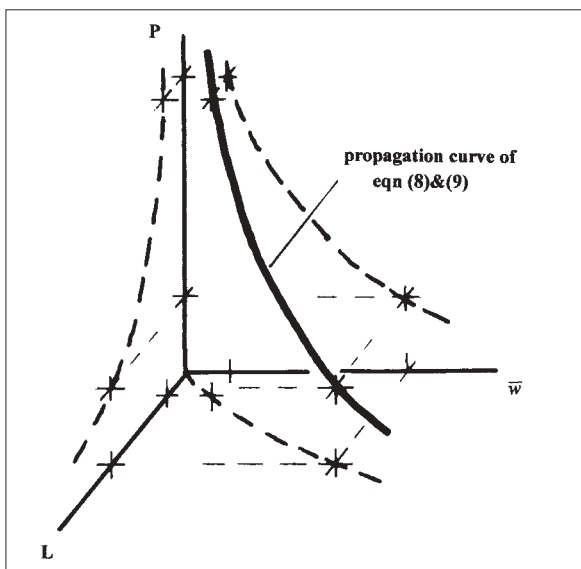


Fig 3. Propagation uplift buckling of a geometrically perfect, restrained column

for the upheaval case of Fig 1(a) these will be given as

$$\bar{w}_1 = -\frac{1}{384} \frac{qL^4}{EI} ; P_c = \frac{4\pi^2 EI}{L^2} \quad \dots(2)$$

whereas for the first of the lateral modes of Fig 1(b), when ξ is the coefficient of lateral kinematic friction between the column and the foundation, they will be given by

$$\bar{w}_1 = -\frac{2.080}{384} \frac{\xi qL^4}{EI} ; P_c = \frac{2.042\pi^2 EI}{L^2} \quad \dots(3)$$

For large L the situation will be reversed. At some intermediate level of L the load P required to sustain the level of deformation, will reach a minimum; this will represent the preferred wavelength, or propagation wavelength, L_p , at this level of deformation, shown schematically in Fig 2(b). Rearranging eqn (1) in the form

$$P = P_c \left(1 + \frac{\bar{w}}{L} \right) \quad \dots(4)$$

and noting that independent of mode shape

$$\frac{dP_c}{dL} = -2 \frac{P_c}{L} ; \frac{d\bar{w}}{dL} = 4 \frac{\bar{w}}{L} \quad \dots(5)$$

the condition for the minimum load

$$\frac{dP}{dL} = 0 \quad \dots(6)$$

will result in the solution being given by

$$\bar{w} = +\bar{w}_1 ; P_p = +2P_c \quad \dots(7)$$

In other words at a given level of uplift deformation the wavelength will be that which makes the downward loading imperfection equal to this deformation. This will occur at a load that is twice the critical load corresponding to this wavelength. Making use of eqn (2) this means that for the upheaval case of Fig 1(a) the propagation envelope of Fig 2(a) will be defined as

$$P_p = 4.029 \left[\frac{EI \cdot q}{\bar{w}} \right]^{0.5} ; L_p = 4.427 \left[\frac{EI \cdot \bar{w}}{q} \right]^{0.25} \quad \dots(8)$$

while for the first of the lateral modes of Fig 1(b), for which the kinematic lateral friction coefficient is taken as ξ , use of eqn (3) will give a propagation envelope defined as

$$P_p = 2.965 \cdot \left[\frac{EI \cdot \xi q}{\bar{w}} \right]^{0.5} ; L_p = 3.686 \cdot \left[\frac{EI \cdot \bar{w}}{\xi q} \right]^{0.25} \quad \dots(9)$$

That these expressions represent approximations of the exact behaviour is the result of taking the lateral deformation of the column under its self weight or friction force as being equal to the imperfection in the lowest critical mode. This is not the case. The lateral deflections are 4th order polynomial functions while the critical buckling mode is a transcendental function appropriate to the boundary condition. However, the shapes of these different modes are so close that the approximation is very minor. In the case of the lateral buckling a further approximation has been introduced by the use of the effective length $0.7L$ for the critical mode of the column. For interest, the exact value for the case of the upheaval mode of Fig 1(a) was developed by Martinet¹ and later Kerr², and in a somewhat more accessible form by Hobbs³, and is given by

$$P_p = 3.962 \left[\frac{EI \cdot q}{\bar{w}} \right]^{0.5} ; L_p = 4.515 \left[\frac{EI \cdot \bar{w}}{q} \right]^{0.25} \quad \dots(10)$$

Eqn (8) can be seen to provide excellent approximations of these more exact expressions.

Fig 3 shows the propagation locus defined by eqn (8) and (9). As the deformation tends to zero the propagation load tends to infinity at a wavelength that also tends to zero. For a column lying on a perfectly flat foundation, the theoretical primary response is that of the column remaining perfectly straight for all values of axial load, P . This raises the not insignificant question as to how the system can ever get onto

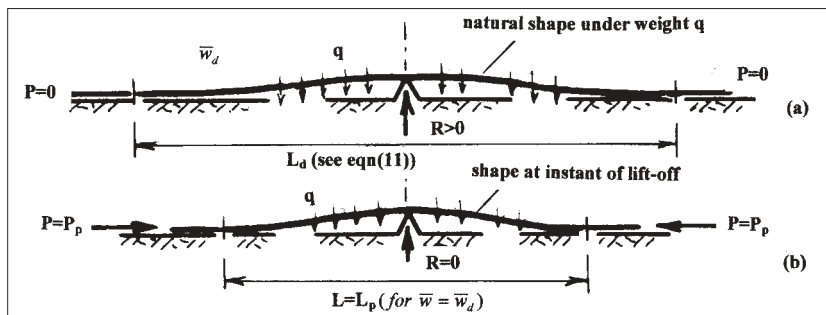
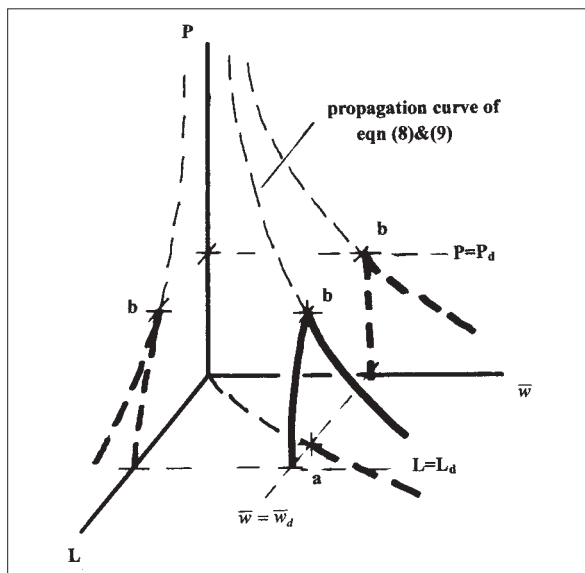


Fig 4. (Above) Form of a column unstressed when straight (a) laid over a rigid discrete protrusion, and (b) the axial shortening due to application of axial load

Fig 5. (Left) Buckling behaviour of a restrained column with an initial discrete imperfection



the propagation path shown in Fig 3?

Role of geometric imperfections

While the above alternative way of modelling the classical restrained thermal buckling of columns is interesting it really adds little to what has been known for a considerable time. Where it becomes very useful however, is in the modelling and interpretation of the way the systems respond in the presence of imperfections. And since the mechanism for the column being able to get onto the propagation curve of Fig 3 is all to do with initial geometric imperfections, this alternative modelling takes on a particular importance. The imperfections can take a variety of forms.

Discrete imperfection: The simplest form of imperfection is that shown in Fig 4. When a straight column is laid upon a foundation with such a discrete high point it will take-up a unique shape having a wavelength L_d given by

$$L_d = 5.826 \cdot \left[\frac{EI \cdot \bar{w}_d}{q} \right]^{0.25} \dots(11)$$

This can be seen to be somewhat longer than the propagation wavelength of eqn (8) for a deformation of this magnitude. As axial compression is increased, as a result of heating, the regions of sagging will experience additional downward forces tending to push them back onto the foundation. This would result in a shortening of the length of column lifted above the foundation. Hogging regions will have an upward force that eventually becomes great enough to lift the column off its discrete central support. When this happens, the column will be unaware that it started from the imperfect geometry and the state of equilibrium will be identical to that of the propagation curve of Fig 3. Buckling will occur at point 'b' in Fig 5 where

$$P_d = 4.029 \cdot \left[\frac{EI \cdot q}{\bar{w}_d} \right]^{0.5} \quad L_d = 4.427 \cdot \left[\frac{EI \cdot \bar{w}_d}{q} \right]^{0.25} \dots(12)$$

Because the process of shortening the uplifted wavelength will have resulted in a small axial lengthening, the temperature required to induce this uplift will be a little greater

than $T_d = P_d / \alpha AE$, where α is the coefficient of thermal expansion of the column having extensional stiffness AE . It is worth noting that at this temperature a sudden snap buckling will occur, with the eventual amplitude of the buckled column being partly governed by the friction coefficient over the length of column still in contact with the foundation. Further discussion of the relationship between the axial force and the temperatures during buckling will be left to later.

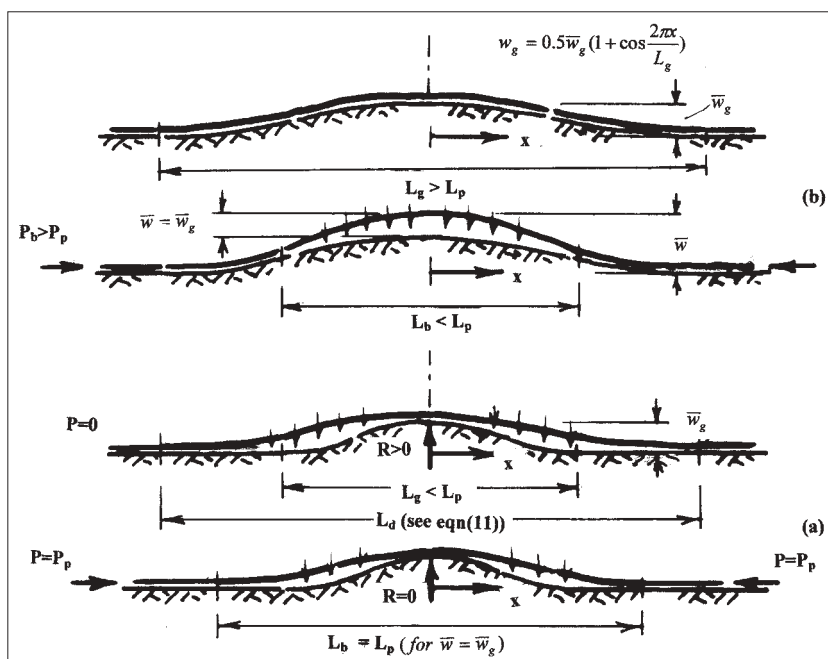
Continuous imperfection (stressed): If an unstressed straight column is laid upon a foundation that is not flat, the column will be forced to take-up the shape of the foundation as shown in Fig 6(b). Before any thermally induced compression is introduced the column will therefore contain bending stresses consistent with the shape into which it has been forced. In this case the buckling behaviour will depend upon the nature of the foundation undulation. For simplicity, and because it corresponds with the most critical shape, it will be assumed that the foundation has a form

$$w_g(x) = 0.5\bar{w}_g \left(1 + \cos \frac{2\pi x}{L_g} \right) \dots(13)$$

shown in Fig 6, to be similar to that of the uplift buckle. Since this class of stressed geometric imperfection is unlikely to arise for the case of lateral buckling, the discussion of this section is confined to just upheaval buckling. The buckling behaviour will strongly depend upon the wavelength, L_g , of the geometric imperfection.

For $L_g < L_p$, as depicted in Fig 6(a), (where L_p is taken to be the wavelength for the propagation load that would occur for a displacement equal in magnitude to \bar{w}), the column when laid will be in only partial contact with the foundation; separation zones will be formed at each of the ends, as indicated in Fig 6(a). As the axial force is increased the sagging region over the separation zone will be forced downwards until the length between the end lift-off points equals L_p . The load required for the overall separation length to reach L_p will be the P_p associated with the imperfection amplitude \bar{w}_g , and the behaviour will be essentially the same as that shown in Fig 5. Indeed, for the shape of geometric imperfection assumed in eqn (13), an initial separation zone at the ends will occur for imperfection wavelengths greater than L_p , but less than a certain critical length when separation for the axially unloaded column ceases to occur. However, for all wavelengths $L_g > L_p$ the behaviour, as shown in Fig 6(b), will be similar. After an initial lift-off at the centre of the column the wavelength will increase with increasing axial load P . During this behaviour the column has essentially two imperfections working against one another. An upward geometric

Fig 6. Form of a column unstressed when straight laid over a rigid continuous imperfection having (a) $L_g < L_p$, and (b) $L_g > L_p$, showing buckling wavelengths L_b when subject to axial load



imperfection is caused by the upwardly buckling clamped column having a small slope imposed at its ends where lift-off is occurring; this will initially dominate, since as discussed in for example Reference (4) this geometric imperfection is proportional to the square of the current uplifted wavelength L^2 . In contrast, the downward loading imperfection, resulting from the weight of the column acting over the uplifted zone, is as shown in eqn (2) proportional to L^4 . For short uplift wavelengths the upward geometric imperfection will dominate with the resulting stiffness being positive. As L increases the loading imperfection will become larger at a greater rate than the geometric imperfection with the result that eventually the two are in perfect balance. When this occurs, the equilibrium paths being followed will switch from the primary paths having positive slope to the complementary paths having negative slope. The transition between these two equilibrium paths provides the maximum point on the equilibrium path. It occurs when the column is acting like a perfect column for which the load will be given by the critical load for the wavelength at which these two imperfections balance each other out. It is possible to derive analytic expressions for the wavelength corresponding to the zero total imperfection^{4,5}, and hence obtain simple analytical expressions for the associated buckling loads. However, if the interest is in the lowest possible buckling load for a given imperfection amplitude then it really is not necessary to do so. For all wavelengths $L_g > L_p$ the geometric imperfection at a given uplift wavelength L will be smaller than that occurring when $L_g = L_p$. It follows that the wavelength for which the loading imperfection will exactly balance this upward geometric imperfection will also be smaller than when $L_g = L_p$. This in turn means that the critical load for this wavelength, and hence the buckling load shown in Fig 7, will be higher than for the case of $L_g = L_p$. For a geometric imperfection that has been forced into what was an unstressed column when straight, the lowest buckling load for a specified level of out-of-straightness \bar{w}_g , is therefore

$$P_b = P_g = 4.029 \cdot \left[\frac{EI \cdot q}{\bar{w}_g} \right]^{0.5} \quad \dots(14)$$

This can be seen from eqn (12) to be identical to the uplift buckling of a column having a discrete imperfection.

Continuous imperfection (unstressed): While the above situation would be relevant to a pipeline being laid upon a seabed which has say a hard rock protrusion or undulating profile, it is possibly not so relevant to a railway track potentially undergoing a lateral buckle, and certainly of no relevance to a concrete road pavement when experiencing an upheaval buckling. A concrete road pavement if poured into an uneven sub-grade will, when cured, not contain the bending stresses that would otherwise be associated with the uneven shape. So the following is of definite importance to road pavements and conceivable importance to railway tracks undergoing thermally induced buckling. Again, the nature of buckling will be dependent upon the wavelength of the imperfection, L_g .

Fig 8 shows three cases of L_g relative to the propagation wavelength L_p (again associated with the amplitude \bar{w}). Fig 8(a) shows the rather special situation occurring when $L_g = L_p$. Initial lift-off at the centre of the imperfection will commence when the out-of-balance force produced by the axial force P acting on the curvature of the imperfect column, given by eqn (13) evaluated at $x = 0$, is just equal to the weight of the column, q . This condition will occur when

$$P_L = \frac{2\pi^2 \cdot EI}{L_p^2} \quad \dots(15)$$

which can be seen to be exactly quarter the propagation load associated with this wavelength. As for the case of the stressed geometric imperfection discussed above, the lift-off length will gradually increase with a positive but decreasing stiffness. The stiffness will again go to zero when the downward loading imperfection is equal but opposite to the

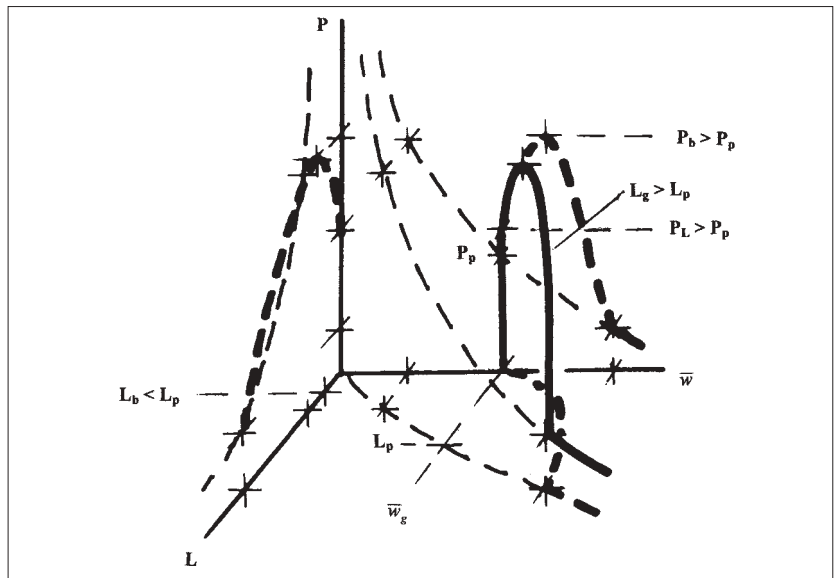


Fig 7. Buckling behaviour of a restrained column with an initial continuous geometric imperfection having $L_g > L_p$

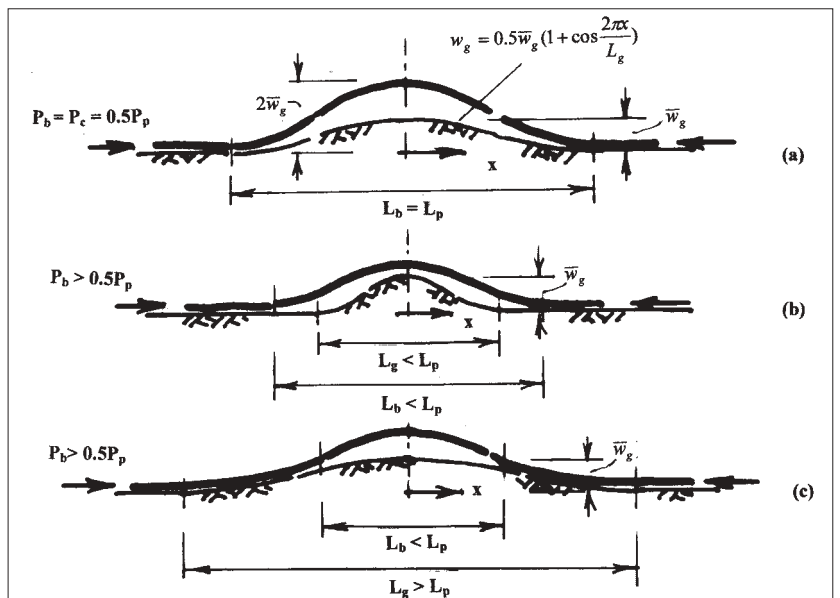
upward geometric imperfection. This situation will arise when the lift-off length just reaches L_p , and will occur at the critical load associated with the wavelength L_p . That is the imperfection sensitive buckling load will be

$$P_b = P_c = \frac{4\pi^2 \cdot EI}{L_p^2} \quad \dots(16)$$

which is exactly half the propagation load P_p that would occur for a displacement equal to \bar{w} , and twice the initial lift-off load P_L . Furthermore, the buckling state will have an incremental displacement that is exactly equal to the amplitude of the initial imperfection, or, put another way, the total deformation will be twice that for the equivalent propagation state. This level of deformation ensures, at least to within the approximation inherent within the current approximate modelling, that the bending moments at the lift-off positions at the end of the buckled region are zero. In the more exact modelling outlined in for example Ref 5 the criterion for the definition of the propagation condition of eqn (6) gives rise to an exact satisfaction of the zero moment condition at the lift-off points. In the classical approach to the definition of the propagation state the third boundary condition of zero moment, in addition to the kinematic requirements of zero displacement and slope, is used to specify an eigenvalue problem from which the solution given by eqn (10) emerges^{1,3}.

Fig 8(b) shows the case of $L_g < L_p$. Because of the high curvature of the imperfection at the centre, an initial lift-off will occur at a relatively low load. While the uplifted wavelength is less than L_g the geometric imperfection will be

Fig 8. Form of restrained buckling modes of a column unstressed when laid over a rigid continuous imperfection having (a) $L_g = L_p$, (b) $L_g < L_p$, and (c) $L_g > L_p$



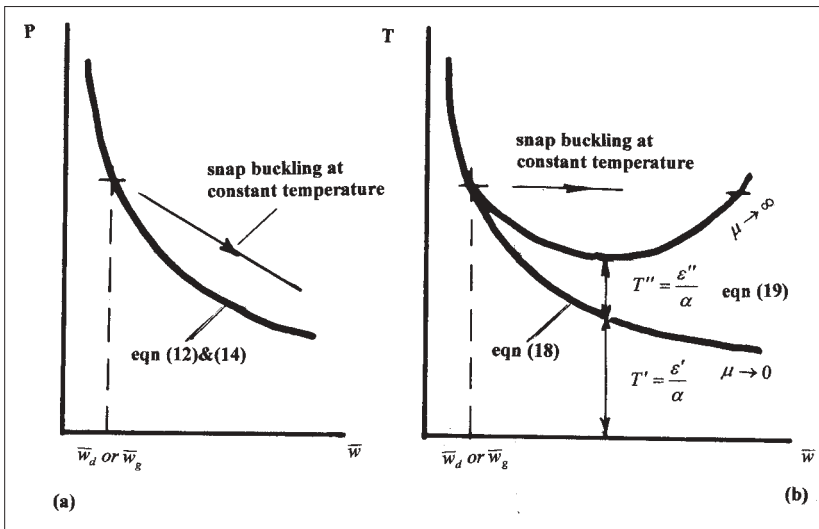
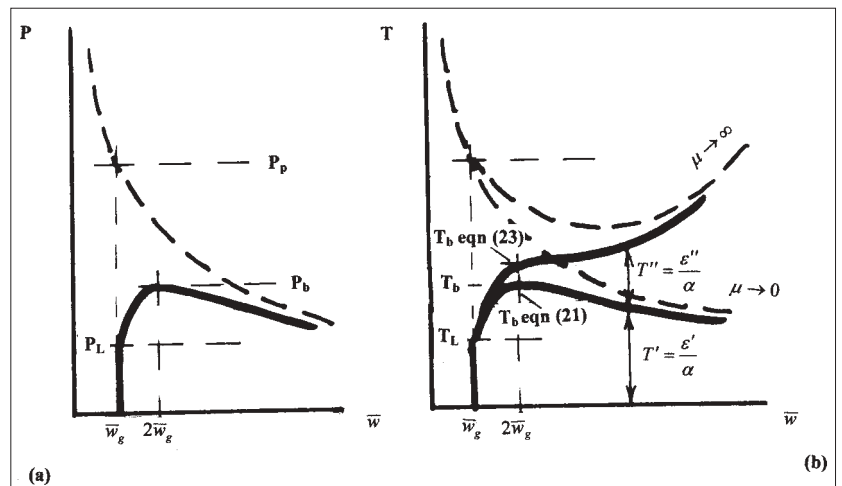


Fig 9. Buckling behaviour of a restrained column stressed when laid over a discrete geometric imperfection, showing (a) propagation load, and (b) propagation temperatures for extremes of longitudinal kinematic friction coefficient

Fig 10. Buckling behaviour of a restrained column unstressed when laid over a continuous geometric imperfection, showing (a) load, and (b) temperature against uplift deformation for extremes of longitudinal kinematic friction coefficient



considerably greater than the downward loading imperfection, so that the load displacement response will have a positive slope. Buckling will occur in these circumstances only after the uplift length has extended beyond the imperfection zone. This will mean that at the wavelength when buckling eventually occurs the original geometric imperfection will be effectively much smaller than the original amplitude, \bar{w} . This will in turn mean that the wavelength L_b at which the geometric imperfection is exactly counterbalanced by the loading imperfection, will be smaller than that associated with the propagation wavelength L_p . Since the buckling load is the critical load associated with a clamped column having this shorter wavelength, it follows that buckling will occur at a load that is higher than that associated with the case of $L_g = L_p$. Wavelengths of geometric imperfections shorter than L_p are consequently not critical for design.

The situation is similar for geometric imperfections having wavelengths that are greater than L_p . This is depicted in Fig 8(c). Because the curvature at the centre of the imperfection is less than that for $L_g = L_p$, the initial lift-off will occur at a load higher than the lift-off given by eqn (15). As the lift-off zone extends the geometric imperfection, governed by the slope at the points of lift-off, will be less than that for the case of $L_g = L_p$. This implies that the wavelength at which the downward loading imperfection becomes equal to the upward geometric imperfection, will also be less than that required for $L_g = L_p$. Once again the buckling load, which is the critical load associated with this zero total imperfection wavelength, will be greater than that occurring when $L_g = L_p$. This means that the least possible buckling load for a specified amplitude of out-of-straightness, will be that given by eqn (14) which corresponds with the imperfection wavelength L_b given by

$$P_b = 0.5P_p = 2.015 \cdot \left[\frac{EI \cdot q}{\bar{w}_g} \right]^{0.5}; L_b = 4.427 \cdot \left[\frac{EI \cdot \bar{w}_g}{q} \right]^{0.25} \dots(17)$$

Buckling temperatures

Most of the above discussion has centred on the axial loads required to induce restrained buckling, it being understood that the compression results from the axial constraint to any expansion that would otherwise occur when the column temperature is increased. Where little or no lateral deformation occurs prior to buckling the temperatures required can be taken directly from $T = P/\alpha AE$. This means for example, that the temperature T_d for buckling from a discrete prop, or the worst possible wavelength for a stressed continuous geometric imperfection T_g , could be approximated by

$$T_d = \frac{4.029}{\alpha AE} \cdot \left[\frac{EI \cdot q}{\bar{w}_d \text{ or } \bar{w}_g} \right]^{0.5} \dots(18)$$

These expressions ignore the small tensile strains that would be developed over the buckled region as a result of the small lateral displacements occurring while the length of the separation zones are decreased prior to buckling. Because

any tensile strain induced would require a slightly higher temperature, the expression of eqn (18) will be slightly conservative. The only major impact of the effects of lateral displacements in these cases will be in controlling the advanced post-buckling response. They will, as suggested in Fig 9(b), govern the displacement and the eventual wavelength taken-up after the snap buckling that takes place at constant temperature. While knowledge of this post-bucked state may be important in certain situations, for example in being able to assess whether material failure might occur during buckling, it is assumed here that the aim is to prevent buckling from occurring. That being the case the expression of eqn (18) is all that is needed.

This is not the situation for the buckling from a stress free geometric imperfection. In this case Fig 10(a) shows that possibly significant lateral deformations will have occurred prior to the maximum load being reached. These lateral deformations will induce a non-linear tensile strain given by

$$\epsilon'' = \frac{1}{L} \left[\int_{-0.5L_g}^{+0.5L_g} 0.5 \left(\frac{dw}{dx} \right)^2 dx - \int_{-0.5L_g}^{+0.5L_g} 0.5 \left(\frac{dw_g}{dx} \right)^2 dx \right] \dots(19)$$

(see Fig 8 for notation), which, for modes assumed to be in the form of eqn (13) and ignoring terms of higher order than quadratics in displacement, yields

$$\epsilon'' = \frac{\pi^2}{4} \cdot \left[\left(\frac{\bar{w}}{L} \right)^2 - \left(\frac{L_g}{L} \right) \left(\frac{\bar{w}_g}{L_g} \right)^2 \right] \dots(20)$$

Along with the membrane strain $\epsilon' = P/AE$ these non-linear strains will contribute to the temperature required to produce buckling. Since space does not permit a more extensive discussion of friction effects, just two extreme cases are considered.

If the longitudinal friction coefficient is zero, $\mu = 0$, then energy will be feed into the buckling zone over an infinite length of the column either side of the buckle. This means that whatever is the level of ϵ'' the axial force and temperature will be related through $T = P/\alpha AE$. This results in the lower equilibrium path shown in Fig 10(b). In particular the buckling temperature will conservatively be given by

$$T_{b0} = T_g = \frac{2.015}{\alpha AE} \cdot \left[\frac{EI \cdot q}{\bar{w}_g} \right]^{0.5} \dots(21)$$

At the other extreme is an infinite friction coefficient, $\mu = \infty$. In this case an equilibrium path will increasingly diverge from that associated with zero friction. Where it exhibits a maximum the buckling temperature will occur at a somewhat larger deformation than that producing the maximum load, and consequently at a higher temperature. However, if a conservative design estimate is needed then to take the temperature at the deformation corresponding with the peak load P_b should provide a fairly reliable but safe estimate of the more exact peak buckling temperature. Recalling that the peak load P_b occurs at a deformation twice that of the imper-

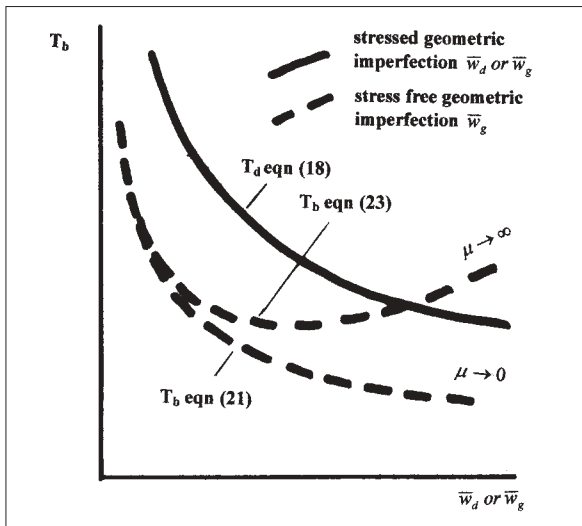


Fig 11. Sensitivity of maximum, buckling, temperatures to stressed and unstressed continuous geometric imperfections, for extremes of kinematic friction coefficient

fection amplitude, and with a wavelength equal to the propagation wavelength, the non-linear strain of eqn (20) will be

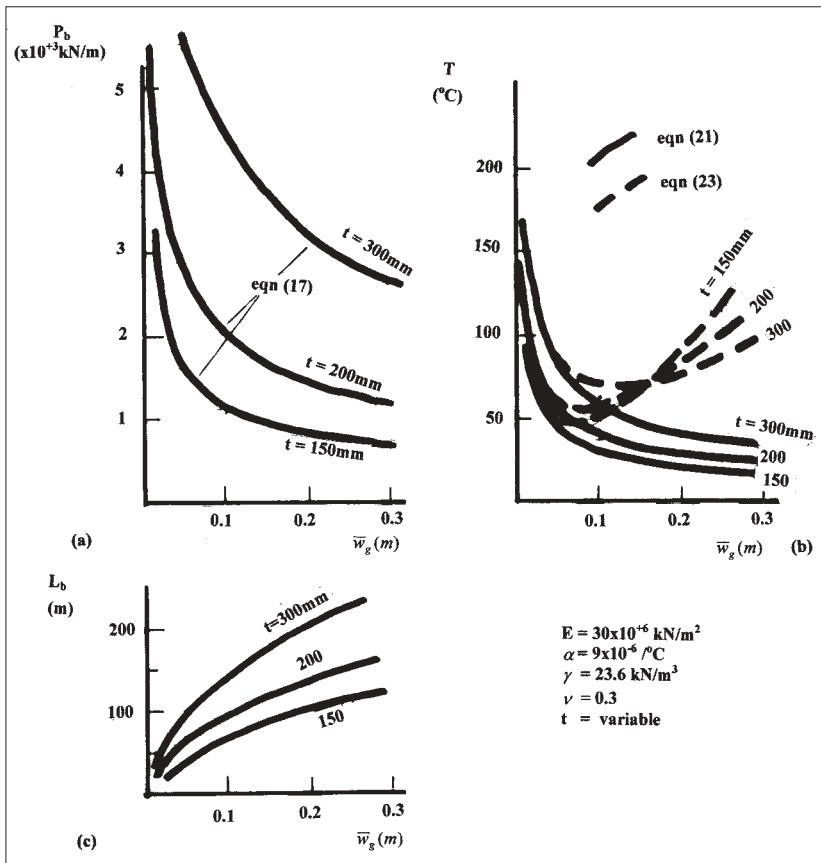
$$\epsilon^r = \frac{3}{4} \cdot \left(\frac{\pi \bar{w}}{L_p} \right)^2 \dots(22)$$

and consequently the lower bound to the actual buckling load is

$$T_{b\infty} = T_g = \frac{1}{\alpha} \cdot \left[\frac{2.015}{AE} \cdot \left(\frac{EI \cdot q}{\bar{w}_g} \right)^{0.5} + 0.378 \cdot \left(\frac{\bar{w}^3 \cdot q}{EI} \right)^{0.5} \right] \dots(23)$$

These expressions are depicted in Fig 11 in the form of imperfection sensitivity plots. It needs to be remembered that for a given level of imperfection these plots represent the choice of associated wavelength that would produce the most severe reduction in buckling temperature; for this reason they provide lower bound predictions of buckling. It is clear that for unstressed geometric imperfections the importance of longitudinal friction coefficient increases as the level of imperfection increases.

Fig 12. Sensitivity of (a) buckling loads, (b) buckling temperatures, and (c) buckling wavelengths for unstressed continuous geometric imperfections in concrete road pavements



Some typical examples

To illustrate the orders of magnitude involved, examples will be chosen from two different but nevertheless practically very relevant fields.

Concrete road pavements: Fig 12 shows typical imperfection sensitivity plots for upheaval buckling of three examples of concrete road pavement. Assuming an unstressed continuous imperfection having an amplitude \bar{w} in the critical wavelength shown in Fig 12(c), the buckling loads P_b , expressed as force per unit width of pavement and the buckling temperature T_b for two extremes of longitudinal kinematic friction μ are shown in Figs 12(a) and (b). With low friction coefficients and moderate levels of out-of-flatness, the increases in temperature required to produce uplift buckling are for certain pavement thicknesses well within the ranges of seasonal variations experienced within the UK. The vulnerability to uplift buckling increases as the pavement thickness is decreased. At high levels of imperfection the buckling temperatures are observed to have a high level of sensitivity to the precise value of the longitudinal frictional coefficient, with the sensitivity increasing as the pavement thickness decreases. Interestingly, for high longitudinal friction coefficients, the buckling temperatures exhibit a minimum at a particular amplitude of geometric out-of-flatness. This minimum depends upon the level of the longitudinal friction. It is clear that thermal uplift of rigid concrete pavements should be considered as part of the normal design process. Where it is not considered, or where the expansion joints fail to act properly, the results can be dramatic⁶, and more recently in the damage caused to the motorway network in the UK⁷. It might be remarked that as a result of the serious deterioration experienced in many of the UK's concrete motorway pavements in the vicinity of the expansion joints, it has become increasingly common practice to cast the pavements continuously and without expansion joints. In these circumstances it is even more important that thermal buckling considerations should be taken into account when designing and constructing rigid road pavements⁸.

Steel railway track: As an example of lateral buckling the two-lobe wave of Fig 1(b) is considered. For a continuous, stress free, out-of-straightness taking the same form as this buckling deformation, the initiation of lateral deformation will from eqn (9) occur at

$$P_L = 0.25P_p = 0.741 \left[\frac{EI \cdot \xi q}{\bar{w}_g} \right]^{0.5} \dots(24)$$

while the maximum buckling load will be given by

$$P_b = 0.50P_p = 1.483 \left[\frac{EI \cdot \xi q}{\bar{w}_g} \right]^{0.5} \dots(25)$$

For the two extremes of longitudinal friction coefficient a lower bound to the buckling temperatures will be given as

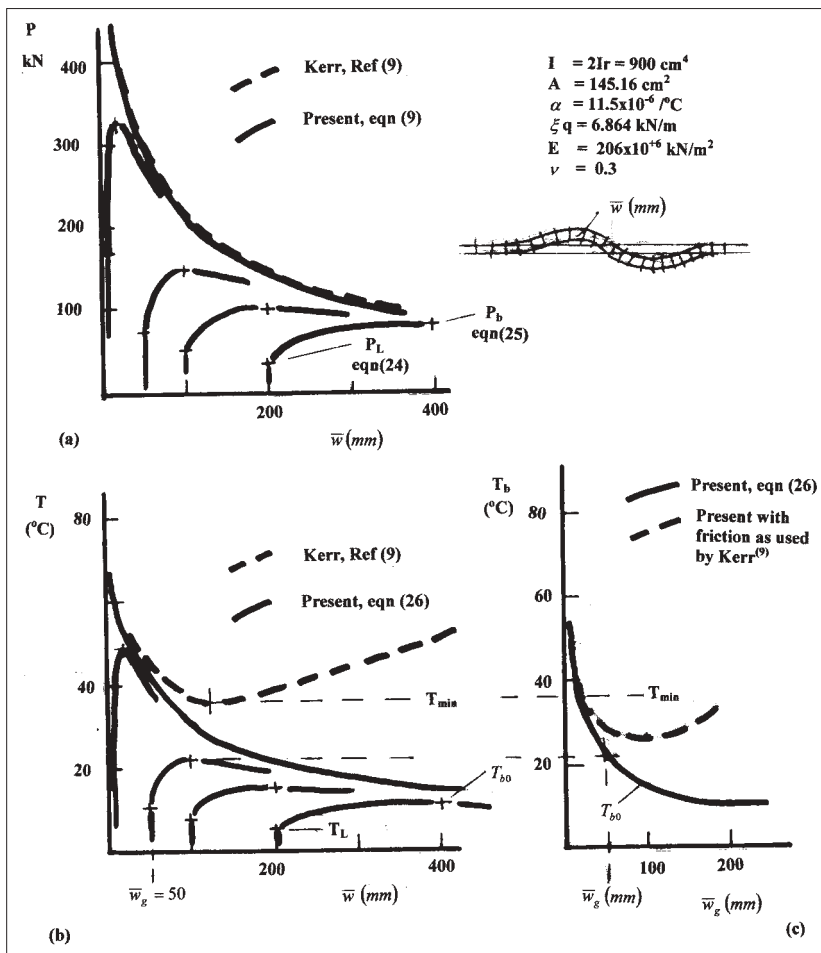
$$T_{b0} = T_g = \frac{1}{\alpha} \cdot \left[\frac{1.483}{AE} \cdot \left(\frac{EI \cdot \xi q}{\bar{w}_g} \right)^{0.5} \right] \text{ for } \mu = 0 \dots(26)$$

and allowing for the differences in mode shape as well as the effects of the nonlinear tensile strains

$$T_{b\infty} = T_g = \frac{1}{\alpha} \cdot \left[\frac{1.483}{AE} \cdot \left(\frac{EI \cdot \xi q}{\bar{w}_g} \right)^{0.5} + 0.671 \left(\frac{\bar{w}^3 \cdot \xi q}{EI} \right)^{0.5} \right] \text{ for } \mu = \infty \dots(27)$$

Fig 13 (a) and (b) show respectively the load and temperature against lateral deformation for a selection of values for the initial out-of-straightness. The parameters chosen for this particular example are those used in Fig 7 of Kerr⁹. For comparison the results reported by Kerr⁹ are also included.

Before commenting upon the practical significance of the results shown a few remarks about the results of Kerr⁹ might be appropriate. The heavy broken curves of Figs 13(a) and (b) are essentially the classic propagation curves which can be seen to closely agree with eqn (9). For the case of the tempera-



ture displacement of Fig 13(b) the minimum T_{min} is the result of the particular characteristics of the longitudinal friction between the track and the subgrade refined over a number of years by Kerr to reproduce measured track conditions. It is reasoned that this minimum temperature is the lowest temperature for which multiple equilibrium states will occur, and consequently it is the lowest temperature for which it is possible to get a snap buckling from one of these states to another. However, this approach fails to explain how in the real system the response will get from the undeformed state onto the classic propagation states at some finite temperature. This transitional situation has been shown to be the result of the inevitable pre-existing geometric imperfections in the track profile. These are not considered in the analysis reported by Kerr⁹ and hence all that his and other contemporaneous analyses could suggest is that buckling cannot occur at temperatures lower than the minimum T_{min} . But unfortunately even this is possibly not true as the current results show.

The nonlinearities of eqn (20) are dependent upon the incremental deformations from the initially imperfect column. The heavy broken line of Fig 13(b), reproduced from the results of Kerr⁹, does not take into account the presence of imperfections and consequently assumes that the nonlinearities arise from the total deformations and not just the changes in deformation. For a stressed continuous geometric imperfection the response will be similar to that shown in Fig 9(b). For an unstressed continuous geometric imperfection, assumed to be relevant to the situation of lateral buckling of rail tracks, the response would take the form shown in Fig 10(b). In either case the deviation between the zero and infinite curves only begins when lift-off commences. An approximate allowance for the effects of incremental nonlinearities on the imperfection sensitive buckling temperatures, for the friction characteristics used by Kerr⁹, is shown by the heavy broken line in Fig 13(c). For very small imperfections the effects of longitudinal friction can be seen to be small. However, even at relatively small imperfection levels the buckling temperatures are suggested

to be lower than the T_{min} reported by Kerr⁹ to provide the lowest temperature for thermal buckling. An imperfection of just 25mm can be seen to result in a buckling temperature a little over 30°C. Because the incremental deformation at this buckling temperature is small the effects of nonlinearities, and hence longitudinal friction, are also seen to be small. While the buckling temperatures become increasingly sensitive to the effects of longitudinal friction coefficient μ as the levels of initial imperfection increase, it is clear that the use of T_{min} could seriously overestimate the temperatures required to trigger the buckling of railway track containing small geometric out-of-straightness. For the present example an imperfection of 50mm will, depending upon the level of the longitudinal friction coefficient μ , trigger buckling at a temperature somewhere between 20°C and 30°C. These results point to a need in railway track design to relate the safe thermal buckling temperatures not only to the lateral and longitudinal friction characteristics between the track and the subgrade, but also to the levels in the geometric tolerances on track alignment taken to be acceptable during the laying of the track.

While the rail parameters adopted by Kerr⁹ relate to track in the USA, it is likely that UK track buckling will exhibit similar features. If so, then the recent spate of track buckles would be consistent with the levels of temperature predicted in Fig 13 to be required for buckling and those that were experienced during the unusually hot summer of 2003.

Concluding remarks

An alternative interpretation of the restrained buckling of columns, appropriate for thermal buckling problems, is shown to make use of the well known buckling of a simple column. This provides an interesting but not overly helpful alternative derivation of the classic, thermal buckle propagation model. When extended to include the effects of geometric imperfections however, this alternative interpretation takes on particular significance. Buckling loads for geometrically imperfect restrained columns can be viewed as the interplay between two imperfections of opposite sign that eventually cancel each other out. With the critical eigenvalue for the column having the wavelength at which this zero total imperfection occurs, representing this maximum buckling load, it is possible to derive particularly simple expressions for the imperfection sensitivity associated with the thermal buckling problem. Furthermore, the alternative approach allows simple heuristic arguments to be invoked for defining the most critical imperfection shape. Selected numerical examples of this imperfection sensitivity for a range of concrete road pavements and a typical railway track, illustrate the potential importance of the phenomenon and consequently the use which could be made of the simple analytical expressions for the prediction of buckling temperatures.

Fig 13. Buckling behaviour showing (a) load, and (b) temperature against lateral deformation for various unstressed continuous geometric imperfection in a typical railway track, and (c) sensitivity of buckling temperatures to varying imperfection amplitudes

REFERENCES

1. Martinet, A.: 'A flambement des voies sans joints sur ballast et rails de grande longueur'. *Revue Generale des Chemins de Fer*, 1936, 55(2), 212-230
2. Kerr, A. D.: 'On the stability of railroad track in the vertical plane'. *Rail International*, Feb., 1974, 131-142
3. Hobbs, R. E.: 'In-service buckling of heated pipelines'. *ASCE J of Transportation Engng.*, 1984, 110, 175-189
4. Croll, J. G. A.: 'A simplified model of the upheaval buckling of subsea pipelines'. *Thin Walled Structures*, 1997, 198, 59-78
5. Croll, J. G. A.: 'A simplified analysis of imperfect thermally buckled subsea pipelines'. *International J of Offshore and Polar Engng.*, 1998, 8, 283-291
6. Kerr, A. D. and Dallis, W. A.: 'Blowup of concrete pavements'. *J. of Transportation Engng.*, 1985, 111, 33-53
7. NCE, 17 June, 1993
8. Croll, J. G. A.: 'Thermal buckling of pavement slabs'. *Transport Journal of the Proc. ICE*, (in press)
9. Kerr, A D.: 'An improved analysis for track buckling'. *International J. Non-linear Mechanics*, 1980, 15, 99-113